Pergamon

NanoStructured Materials, Vol. 10, No. 6, pp. 965-981, 1998
Elsevier Science Ltd

0965-9773/98 $19.00 + .00

PII S0965-9773(98)00130-5

CHARACTERIZATION OF Al_2O_3 COMPOSITES WITH FINE Mo PARTICULATES, I. MICROSTRUCTURAL DEVELOPMENT

Wen-Cheng J. Wei, Sheng-Chang Wang and Feng-Huei Cheng*

Institute of Materials Science and Engineering, National Taiwan University, Taipei, Taiwan 106, ROC
*Now with Team Young Advanced Ceramics Co., Ltd., Taoyuan, Taiwan

(Accepted August 4, 1998)

Abstract *— Alumina based composites containing nano- or submicron-meter Mo grains in the amounts of 20 vol% or less were prepared through a dissolution of molybdenum oxide in ammonium solution, followed by spray-drying, hydrogen reduction and sintering with or without hot-pressing. The properties of alumina/molybdate solutions and the ζ-potential of alumina particles in the solution were measured. By using electron microscopic and quantified X-ray diffraction techniques, the microstructural features and the evolution of Mo particulate in spray-dried powder and sintered bodies were analyzed. The time dependent exponent and activation energy of grain growth of Mo between 600 to 900°C were determined. There is no glassy phase or reaction at the interfaces between Mo/Al_2O_3 of dense composites. Only one coherent interface was found, and the others are incoherent. The results reveal that submicrometric Mo grains may grow by surface diffusion in reduction stage (≤ 900°C) and greatly retard the densification and reduce the grain size of alumina matrix in sintering stage. ©1998 Acta Metallurgica Inc.*

1. INTRODUCTION

Uniformity and fine-grain are two major microstructural requirements for the preparation of ceramic composites with superior properties. In order to achieve ultimate performance, a ceramic composite should start from the stage of powder synthesis. The advantages of the addition of second phase were reported in several aspects, namely the reduction of grain size of the matrix grain, or the improvement of fracture behavior (1,2). However, agglomeration of the second phase induced by inappropriate surface forces is identified to be the major problem for preparing a desired powder mixture, and also for densified composite. In addition, exaggerated grain-growth of the matrix grains during densification or post heat-treatment is reported to be detrimental to the mechanical properties (3).

Alumina is one of the important structural and electronic ceramics. Various metallic secondary phases reported in current literature were added to improve the mechanical properties of alumina. Mo, either in the form of metallic powder, MoO_3, or Mo fibers, was utilized in several

reports (1, 2, 4-6). McHugh *et al.* (1) prepared the admixture of Al_2O_3/Mo from reducing MoO_3 by H_2. They reported that the improvement in the strength of alumina is due to the refinement of alumina grain size by 5 to 6 vol% of Mo. The reduction of the grain size of alumina matrix by adding Mo was later proven again by Rankin *et al.* (4) and Nawa *et al.* (5) to be the major factor responsible for the strengthening of the alumina composites.

Wet chemical processes, including sol-gel, chemical co-precipitation or gel casting, have demonstrated (7) that chemical routes are potentially able to overcome dispersion difficulties in powder mixtures of various fine powders in different natures. But few chemical processes have proven especially useful for the preparation of ceramic powders with submicrometric or nano-metric size, for instance, Stearns *et al.* reported on the Al_2O_3 system doped with SiC (8).

A dissolution of oxide in an aqueous solution to form a state of Mo-species in a molecular scale, then co-precipitation by spray-drying with second constituent alumina could be advantageous for the preparation of fine ceramic composite through chemical route. MoO_3 is dissolvable in ammonium solution, which can be transferred to either crystalline or amorphous molybdate by a controlled drying step (9). The molybdate tends to decompose to form a series of complex transient products, *e.g.* $(NH_4)_2 \cdot 3MoO_3 \cdot 2H_2O$, or subsequently to form MoO_3 at a higher pyrolysis temperature (300-400°C) (10).

The stability of ceramic particles in a solution is greatly dependent upon the surface potential of ceramic particles. Lower viscosity and high stability of suspension result from a strong electric potential, which is a source of repulsive force among the suspended particles. These properties, including viscosity, solid loading and dispersion conditions, strongly influence the characteristics of spray-dried powders (11) and produced ceramic pieces (12).

The spray-drying technique has been used in ceramic industry for several decades because of the convenience of this technique for a continuous fabrication and the adjustment of the agglomerate size (13). It is well recognized that the size, shape and distribution of spray-dried powder are important to mold-filling and compactness during die-pressing, and consequently to the densification of fired parts.

In this research, Mo metal particles are selected as a second phase added into the Al_2O_3 material. The evolution of Mo--starting from the dissolution of MoO_3 in ammonium solution, then the formation of molybdate phase in as-spray-dried granules, and finally the reduction to form Mo grains in the admixture--was investigated. The chemical route was designed to reduce the grain sizes of Mo in Al_2O_3 matrix and to improve the uniformity of the microstructure of the composites. The detail of the microstructural evolution of the Mo-containing phase in each stage is studied.

2. EXPERIMENTAL

2.1 Sample Preparation

MoO_3 powder (99.95% pure, Climax Molybdenum Company., USA) and Al_2O_3 powder (99.7% pure, A-16SG, Alcoa Industrial Chemical, USA) were used as the precursory materials. The MoO_3 powder was first dissolved in 5 wt% ammonia solution, then the alumina powder was dispersed in the solution to form a alumina/molybdate suspension. After being ball-milled for 1 hr and filtered through a 150 mesh screen, the suspension was subjected to spray-drying (BUCHI 190 spray-drier, BUCHI, Switzerland). The formulation of the suspension and the operation conditions of the spray-dryer were optimized (14) so to get the spray-dried powders with a larger

granular size (4.8 μm), wider distribution, high tap density (1.45 g/cm^3) and smaller repose angle (45°).

The spray-dried granules were subjected to H_2 reduction at temperatures between 600 to 900°C . One hour of reduction at 900°C was sufficient to fully transform molybdenum oxides (MoO_3 or MoO_2) to metallic Mo.

The granulated powder for pressureless sintering was first molded by die-pressing at 85 MPa, or followed with cold isostatic pressing (Doctor CIP, Kobel Co., Japan) at a pressure of 250 MPa in cases with 5 or 10 vol% Mo. The pieces were then sintered in an atmosphere-controlled tube furnace vented with a 5% H_2-N_2 gas mixture with temperatures of up to 1600°C.

The granulated powder for hot-pressing was die-pressed first at 30 MPa in a stainless steel die, then moved into a graphite die and fired in the HP furnace (High-multi 5000, Fijidempa Kogyo Co., Japan), which was operated at temperatures from 1200°C to 1450°C and a uniaxial pressure of 30 MPa.

2.2 Property Measurements of Granulated Powder

Zeta-potential of Al_2O_3 suspensions with a solid concentration of less than 100 ppm suspended in molybdate solutions in the concentrations 0.00 M to 0.03 M was measured by a Zeta-potentiometer (Zeta-Meter 3.0$^+$, Zeta-Meter Inc., USA). Specific electric conductance of the suspension was measured by the meter as well. However, the Zeta-potential was not reliable when the conductance of the suspension was more than 4000 μ $\Omega^{-1}cm^{-1}$. Therefore, an electro-kinetic charge analyzer (ECA 2000, Hemtrac System, Inc., USA) was applied to measure the electrophoretic stream current in the suspensions with higher molybdate concentrations of up to 1.00 M. The concentration of molybdenum ions in ammonia water was assured through the analysis of the suspensions by an atomic absorption spectrophotometer (AA, Perkin-Elmer 5000, USA).

Viscosity measurement of the suspensions for spray-drying was conducted using a rheometer (Rotovisco, Haake Co., Germany) operated at 25± 2°C. Physical properties, repose angle and tap density, of the spray-dried granules were determined by a Hall flowmeter to reveal the flow ability and compactability of spray-dried powder. Microstructures and size distribution of the granulated powders were characterized by using scanning electron microscope (SEM, Hitachi S-4 100, Japan) and transmission electron microscope (TEM, JEOL 100CXII, Japan). The powder specimens for SEM observation were prepared by drying the droplets of alcoholic suspension on a carbon-taped SEM stage. The specimens for TEM observation were prepared according to Cheng's thesis (14). In brief, the granulated powder was mixed with G-1 epoxy (Gatan Inc., USA), then the mixture was coated on alumina thin substrates (0.6 mm thick). Five substrates were laminated to form a sandwich block. The block was kept in a tight condition while being placed in an oven for curing at 120°C for 10 min. The block, normally having four layers of granular powder, was then cut into a thin disk (3 mm diameter), followed carefully by grinding to 70-100 μm thickness, and dimpling the center region and ion-milling to reveal the layer of granules/G-1 epoxy at the center of the TEM thin foil.

Crystalline phases of the granulated powder with and without hydrogen reduction were analyzed by an X-ray diffractometer (Philips PW1710, Philips Co., Netherlands), which was operated with Cu K_α radiation, an operation voltage of 30 kV and a current 20 mA. By adapting the Scherrer equation, as shown below, the crystalline size (G) of the Mo in the composite can be estimated.

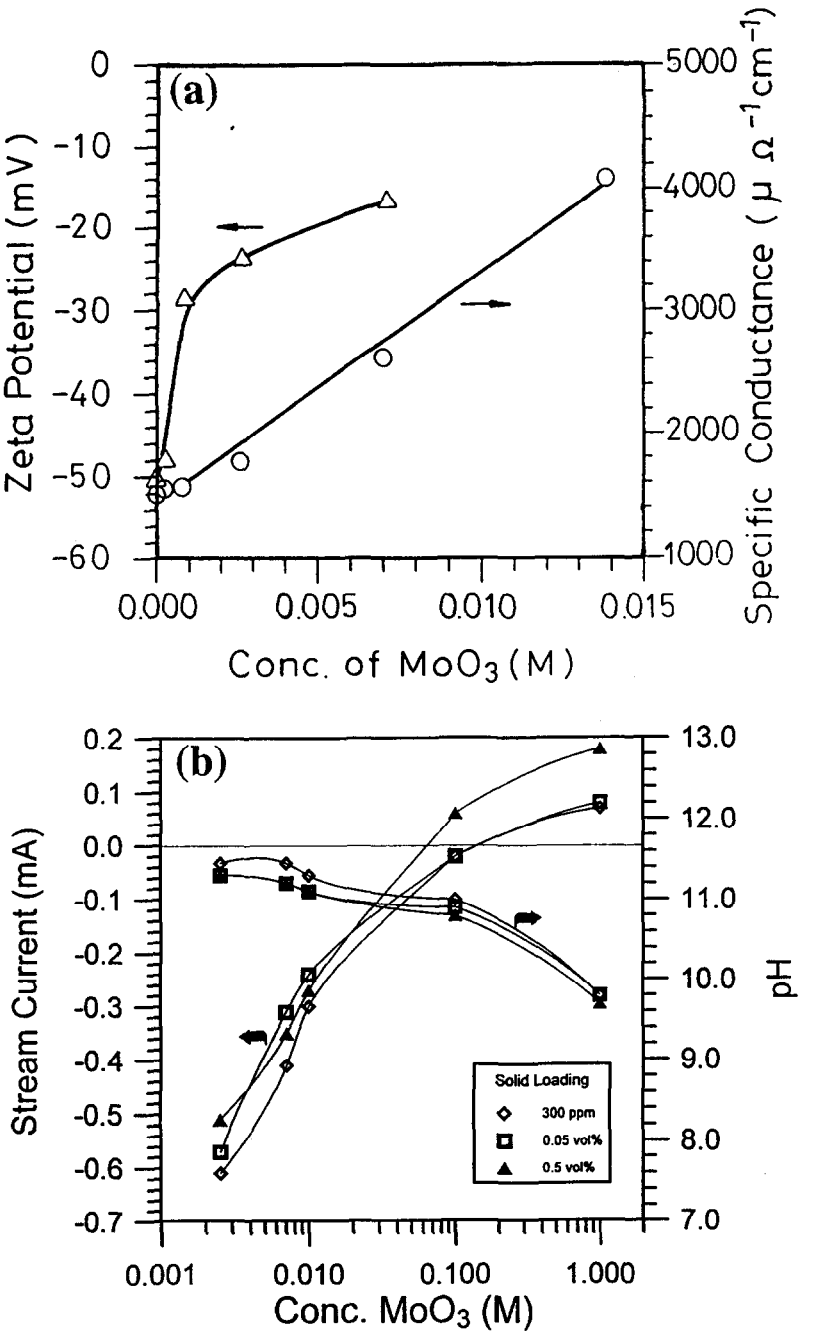

Figure 1. (a) Zeta-potential of Al_2O_3 particles and specific electric conductance, (b) electrophoretic streaming current and pH values of Al_2O_3 suspensions plotted against the concentration of MoO_3 in 5% ammonium solution.

$$G = \frac{K \bullet \lambda}{\beta \bullet \cos\theta} \quad [1]$$

where K is a constant and should be calibrated with specific standard samples (*e.g.* the case shown in Figure 5), β is the half maximum line breadth (HMLB), θ is the diffraction angle of Mo (110) peak, and λ is the wavelength of the incident X-ray. The value of K could be calculated from the crystalline size (G) of Mo measured from any (SEM or TEM) micrographs in different heat-treatment stages. Then the K value would be applied to estimate the G value of Mo in Al_2O_3 under a similar heat treatment.

2.3 Property Measurements of Densified Composite

The granulated powder was firstly die-pressed at a pressure of 30 MPa to form a cylinder in a diameter 6 mm and 5 mm height. Then the cylinder was tested by a dilatometer (Theta Dilatronic II, Theta Co., N.Y., USA) operated in 5%H_2/N_2 atmosphere up to 1250°C in a ramp rate of 5°C/min.

The density of the densified composites was measured by the Archimedes' method. The microstructure of the densified composites was analyzed by either a SEM (Philips 515, Philips Co., the Netherlands) or TEM microscopes (JEOL 100CXII and 4000EX HRTEM, Japan) equipped with a field-emission gun and X-ray energy dispersive spectrometer (EDS). The specimens either for TEM or SEM observation were prepared following the steps referred to that in Cheng's thesis (14). The average grain size and size distribution of Mo or Al_2O_3 were measured by using the linear intercept method (15).

3. RESULTS AND DISCUSSION

3.1 Properties of Alumina Suspensions

The ζ-potentials of Al_2O_3 particles in ammonium molybdate solution and the conductance of the suspension are reported in Figure 1(a). The absolute values of ζ–potentials of alumina are decreasing; however, the conductance of the suspension is linearly increasing as the concentration of molybdate increases. The ζ-potential of Al_2O_3 particles is negative, varying from -50 to -17 mV as the concentration of the molybdate solution is less than 0.007M. The measurement of ζ-potential of Al_2O_3 was very difficult if alumina particles were dispersed in a high-electrolyte solution (> 0.007M molybdate), which would result in a false reading of particle mobility (18).

The isoelectric point (IEP) of high purity Al_2O_3 powder in the range of pH 8.0 to 8.8 is reported in the literature (12). The surface potential of A-16SG powder is in a negative value (-50 mV) in a basic 5 wt% ammonia solution (pH value 11-12). Deprotonation is the cause of the negative surface of the Al_2O_3 particles. However, the absolute value of the surface potential of alumina is decreasing as the concentration of molybdenum oxide increases in the solution, as shown in Figure 1.

There are two types of molybdate ions, MoO_4^{2-} and $Mo_7O_{24}^{6-}$, possibly appearing in an aqueous solution. Luthra (17) reported that MoO_4^{2-} is stable in basic (pH > 7) solution, and would

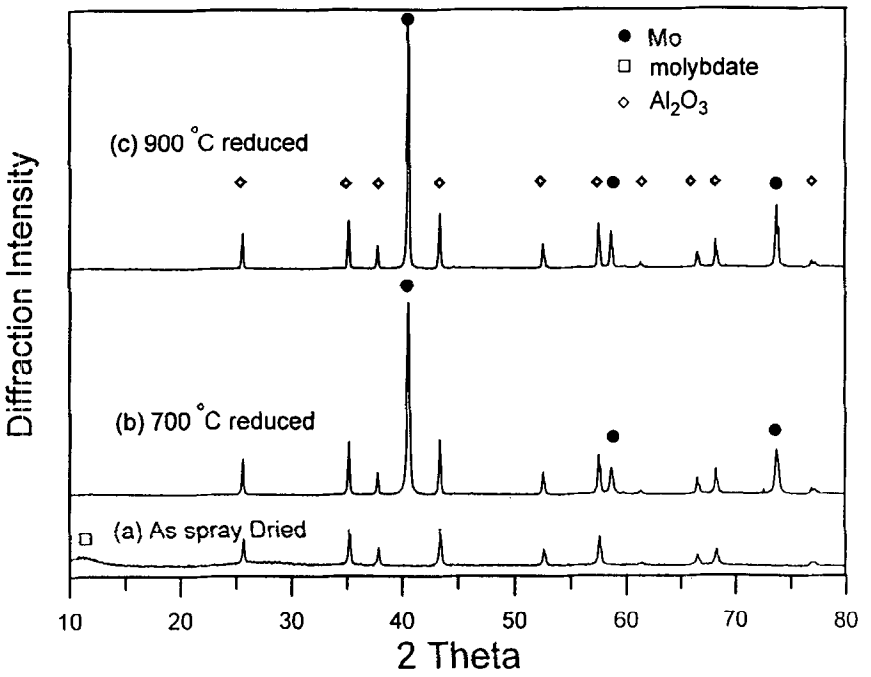

Figure 2. X-ray diffraction patterns of (a) as-spray-dried granules of molybdate/alumina granules, and granules reduced at (b) 700°C for 3 hr and (c) 900°C for 1 hr by pure hydrogen gas.

compete with OH^-, then adsorbed on the alumina surface. As a result, the adsorption of MoO_4^{2-} ions tends to reduce the surface charge of Al_2O_3 particles, and reduces the absolute value of the surface potential of Al_2O_3.

The reading of the stream current and pH of the suspensions at higher molybdate concentrations are reported in Figure 1(b). The results of the stream current, which represents the assembly effects of the mobility and concentration of charged alumina particles, depict a trend of a decrease of negative surface potential as the concentration of molybdenum oxide in the suspension increases. The change of stream current is consistent with the trend of ζ-potential (Figure 1(a)) in similar suspensions. However, a reverse form negative to positive value of the stream current is noted.

According to the report by Modi and Fuerstenau (16), divalent counter ions, *e.g.* sodium sulfite, used as an electrolyte can finally change the sign of the ζ-potential of alumina in solution. The stream current of alumina particles in highly concentrated molybdate solution, as shown in Figure 1(b), changes from negative to positive values as the concentration of MoO_3 is greater than 0.1 M. The reading of the current can be +0.18 mV. The absolute values of the stream current is far less than that in the suspension with a low concentration of MoO_3. This implies that the MoO_4^{2-} ions indeed absorb on the surface of alumina and change the ζ-potential of alumina in molybdate solution with a concentration greater than 0.1 M.

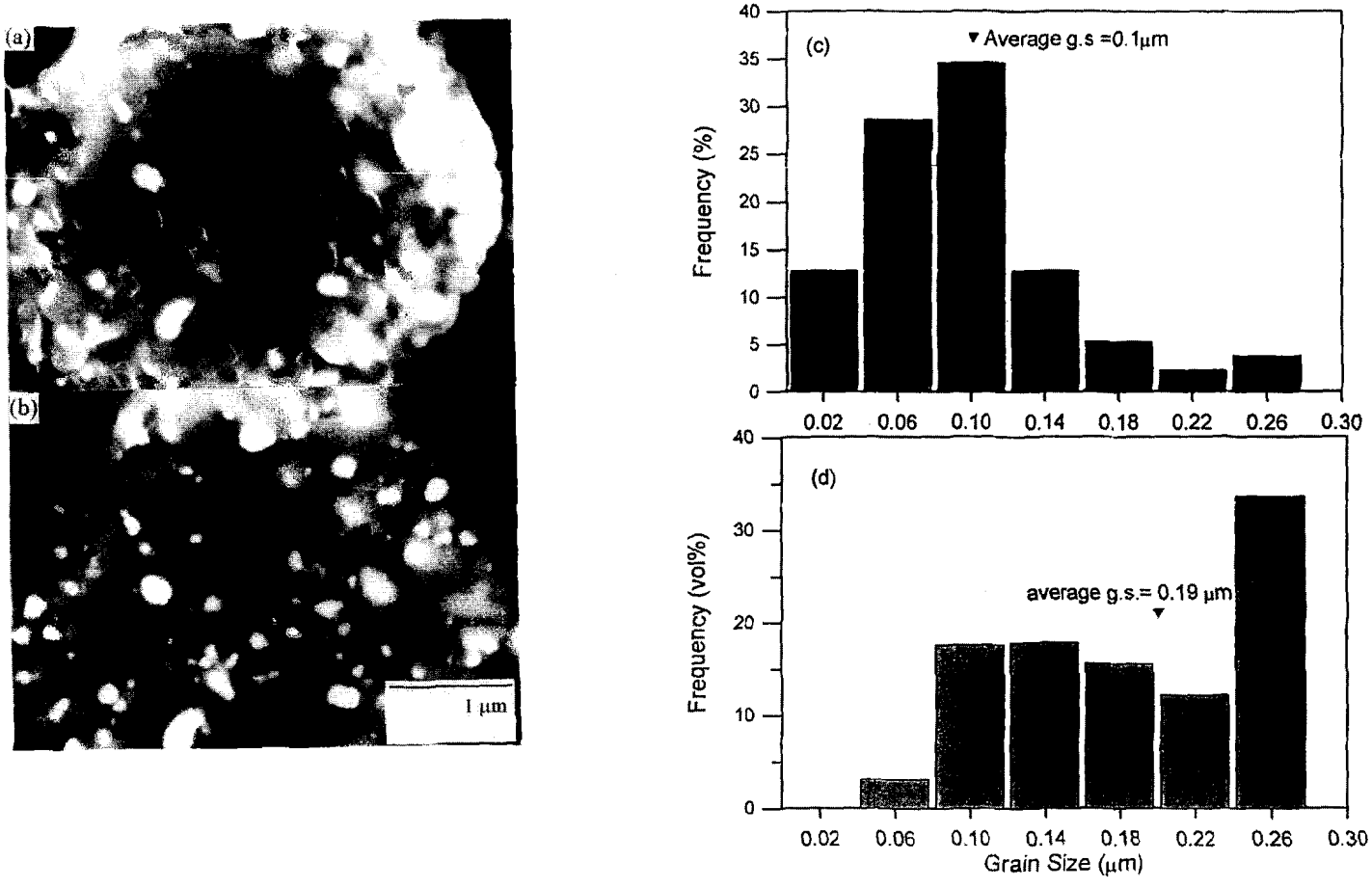

Figure 3. SEM micrographs of one granule reduced at 900°C imaged in (a) SEI mode or (b) BSI mode; and grain size distribution of the 10 vol% Mo/Al_2O_3 granule counted in (c) number or (d) volume percentage.

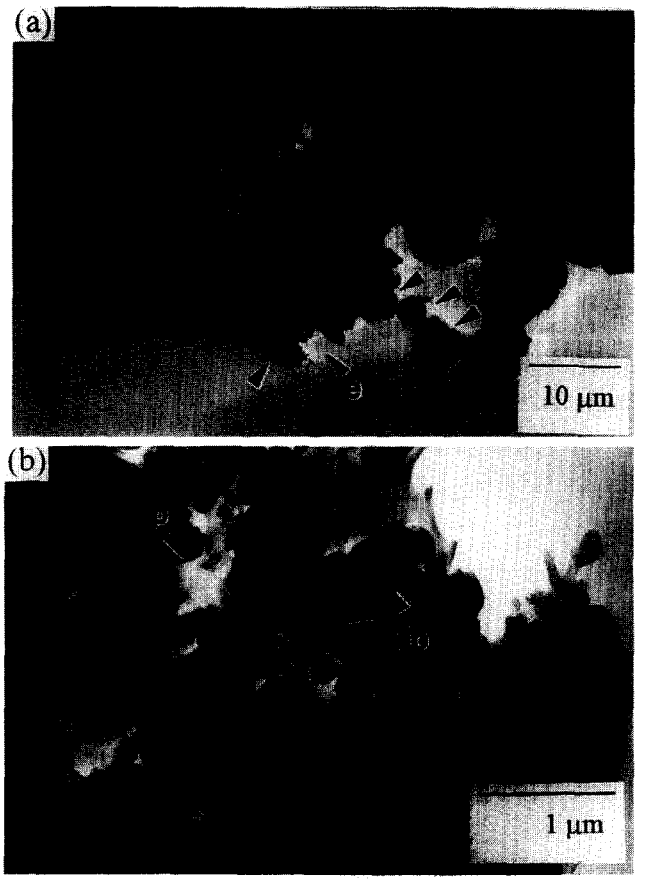

Figure 4. TEM micrographs of (a) the granules and (b) the cross-section of one "e" granule appeared in (a). The granule sample was prepared the same as previous sample. The symbols, g, p and Mo, are discussed in the text.

3.2 Properties of Granulated Powder

The granules of the molybdate/Al_2O_3 composite prepared from the suspensions in 20 vol% solid loading are all nearly spherical. However, the shape of the granules would change to hollow spheres or doughnuts if the solid content in the suspension was reduced. Each granule contains primary submicrometric particles. Crystalline phase identified from their XRD patterns indicates that only crystalline α-Al_2O_3 phase are found in the as-sprayed powder. In addition, a broad diffraction peak between 10° to 13° 2θ angle is pointed out in Figure 2(a), the amorphous ammonium molybdate phase.

The molybdate phase is disappearing starting from 100°C and transforms totally to the MoO_2 phase at 300°C and above. The molybdenum oxide phase can be further reduced in an H_2 atmosphere at 700°C to 900°C to form an Mo metal phase, as shown in the XRD patterns in Figure 2. Mo and alumina phases appear in the 900°C hydrogen reduced composite powder.

Figure 3 is a set of SEM micrographs of hydrogen-reduced composite granule. The micrographs were obtained by two imaging techniques (secondary electron imaging (SEI) and back scattering imaging (BSI)) for emphasis on the surface morphologies of the Mo and alumina grains and on the size and shape of Mo particles on the surface of composite granules. Mo grains in bright contrast were randomly found on the grain boundaries of Al_2O_3. The smallest and largest Mo grains which could be resolved were in a diameter of 0.02 μm or 0.26 μm. The statistical results of the size of Mo grains are shown in Figures 3(c) and 3(d). The average grain size of Mo prepared by H_2 reduction at 900°C is 0.10 μm or 0.19 μm if counted either based on number or volume.

The cross-section of the granules studied by TEM is shown in Figure 4. There are more than three granules (as pointed by "g") transparent to the electron beam. The images of these granules depict that the interior of the granules is not empty. The pores, which are indicated by "p" in the Figure 4(b), have been filled with G-1 epoxy to assure that the porosity is not a result of grain-pull-out during sample preparation, *e.g.* ion milling. Only small pores having sizes of 0.3 μm or smaller are found in Figure 4(b).

Mo grains normally appear in darker contrast than those of Al_2O_3 due to a stronger adsorption of the electron beam by Mo. These tiny dark features in Figure 4(b) could be Mo phase. However, the Mo grains can be assured by the centered dark field (CDF) technique. After a careful comparison of several sets of CDF micrographs, these grains in the figures, indicated as "Mo", are Mo grains.

Figure 5 shows the values of the grain sizes of the Mo phase in alumina granules determined by quantitative XRD and by the previous-mentioned micrographic techniques. The grain size of Mo is in the values of 0.08 to 0.20 μm. But for Al_2O_3, no appreciable change of the Al_2O_3 grain size appears within the range of heat-treated temperatures from 600°C to 900°C.

It was noted that the Mo concentration in the composite powder with 1 vol% Mo through 600°C treatment was hardly detected by XRD due to the concentration of Mo and also due to incomplete reduction. We believe that the average size of the 1 vol% Mo/Al_2O_3 composite should be less than 0.08 μm if reduced at 600°C. The powder (with 1 vol% Mo) also has the smallest Mo size compared to that of the other three powders (5 to 20 vol% Mo/Al_2O_3). The Mo content in the powder formulation does affect the size of the Mo phase for the treatment between 600°C and 900°C.

The composite powder with 10 vol% Mo was selected for the study of grain growth phenomena of Mo. The results of Mo size are plotted against the treated time, and shown in Figure 5(b).

The grain growth of second phase in ceramic matrix as a function of time can be formulated with a power law (19).

$$G^n - G_0^n = k(t - t_0) \qquad [2]$$

where G_0 is the grain size at the initial stage where G_0 is relatively small and can be ignored. The k_0 is a rate constant of grain growth. The n is an exponent of time dependent growth kinetics and can be determined from the reverse value of the slope of the fitted lines in Figure 5(b). It appears that the slopes of the three fitted lines are all close to 0.13 (=1/n), implying that the growth mechanism of Mo grains at 600°C to 900°C in H_2 atmosphere are the same.

In considering the grain growth of Mo in alumina granules, Al_2O_3 grains hardly grow (Figure 5(a)). No coalescence of Al_2O_3 grains takes place to help the growth of Mo grains. In other

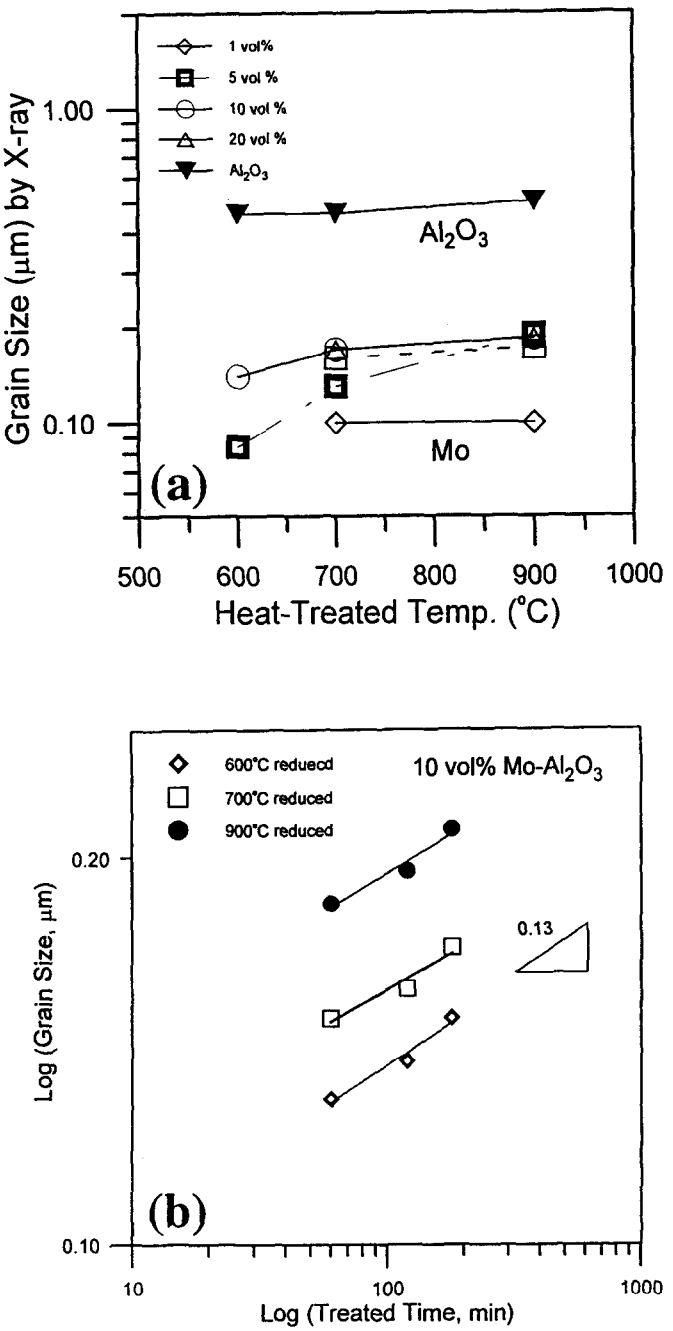

Figure 5. Grain size of Mo of the composites after reduced at specified temperature for 1 hr. (a) Samples with four different contents (either in 1, 5, 10 or 20 vol%) of Mo in Al_2O_3. (b) 10 vol% Mo in Al_2O_3 and treated for various periods.

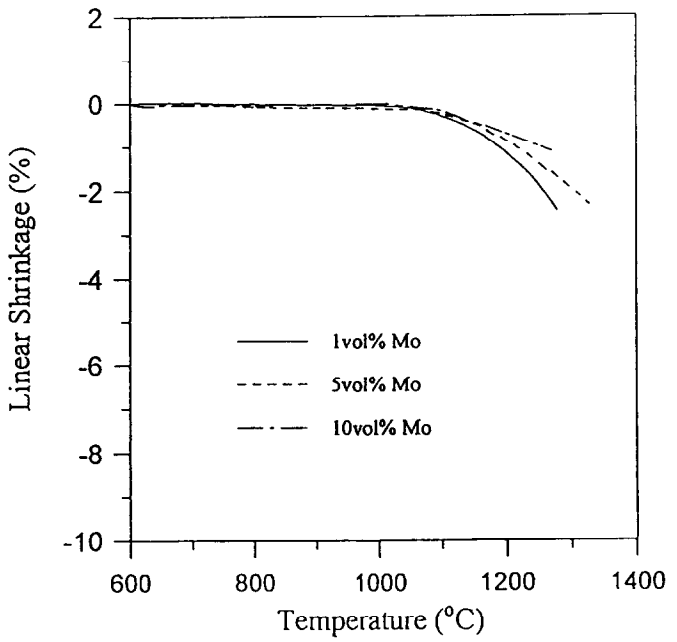

Figure 6. Dilatometric curves of three Mo/Al_2O_3 composites from 600°C to 1250°C at a rate of 5°C /min in 5% H_2/N_2 atmosphere.

aspects of the growing mechanism, the time exponent (n) shown in Figure 5(b) is between 7 and 8. The determined n values are larger than 4 which represents the grain growth mechanism is by the process of Ostwald ripening. Therefore, a surface diffusion mechanism between submicrometric Mo grains is considered. The growth of Mo can be treated analogous to the sintering models discussed by Coblenz *et. al.* (20)

$$(G / G_0)^n \propto \delta D_s \gamma \Omega^m \left(\frac{1}{kT}\right) t \qquad [3]$$

where D_s is the surface diffusion coefficient, δ is the surface layer for diffusion, γ is surface energy, the Ω is the atomic volume for Mo on Al_2O_3 particles occurring in H_2 atmosphere. The time exponent n in equation [3] is in the values of 5 to 7 (19), depending upon the contact shape between particles.

The other interesting issue of Mo grain growth is the role of catalytic effect of alumina to MoO_3. Alumina is a catalysis for the reduction of MoO_3 at temperatures lower than 540°C (21). The reduction rate increases with the decreasing content of MoO_3 on alumina substrate. Sloczynski *et al.* (21) reported that the activation energy associated with the reaction of two types of alumina is either 94±3 kJ/mol or 91±1 kJ/mol. The rate constant k_0 of Mo grain growth (equation [2]) at temperatures 600°C to 900°C is estimated and shown in Table 1. The activation energy of the grain growth is 200 kJ/mol, which is one time greater than that of the reduction reaction. Therefore, the growth of Mo should not relate to the reduction of molybdenum oxide.

TABLE 1
Rate Constant k_0 and Activation Energy of the Grain Growth of Mo Grains during the Treatment in H_2 Atmosphere

	600°C	700°C	900°C	600°C-900°C
k_o (μm/min)	2.75×10^{-3}	4.47×10^{-3}	6.61×10^{-3}	
E (kJ/mol)				200

3.3 Densification and Properties of Composites

Dilatometric curves of the composite powder with Mo contents from 1 to 10 vol% are reported in Figure 6. The threshold of densification of the three samples are all starting from 1100°C. The greater the Mo content is, the slower the densification rate of Al_2O_3 composites will be. Therefore, the sintering temperature of Mo/Al_2O_3 composites was selected to be greater than 1200°C .

The density of the three sets of the Mo/Al_2O_3 composites are shown in Figure 7. The samples were either die-pressed (P.L.) and then sintered in $5\%H_2/N_2$ atmosphere, or cold isostatic pressing (CIP) at 250MPa before 1600°C sintering, or die-pressed then hot-pressed (H.P.) at 30 MPa. The composites with 10 vol% or less of Mo content can be densified at 1 atm to a density of ≥96% T.D. at 1600°C. Similarly, three CIPped composites were sintered at 1600°C. The CIP step only improves by 1% to 2% the theoretical density of the fired density of the composites. The advantage of CIP for the densification of the composites at 1600°C is not apparent. However, hot-pressing can help the composites to fully densify at temperatures of 1350°C or above.

TABLE 2
Average Grain Sizes (μm) of Mo and Al_2O_3 in Mo/Al_2O_3 Composites

Formulation, Mo content	Sintering conditions	Mo	Al_2O_3
1 vol% Mo	1600 °C P.L. in $5\%H_2/N_2$ atmosphere	0.25	4.8
5 vol% Mo	1600 °C P.L. in $5\%H_2/N_2$ atmosphere	0.40	1.4
10 vol% Mo	1600 °C P.L. in $5\%H_2/N_2$ atmosphere	0.65	1.2
10 vol% Mo	HP at 1350 °C in vacuum	0.33	0.62
10 vol% Mo	HP at 1450 °C in vacuum	0.35	0.80
20 vol% Mo	HP at 1400 °C in vacuum	0.28	0.58

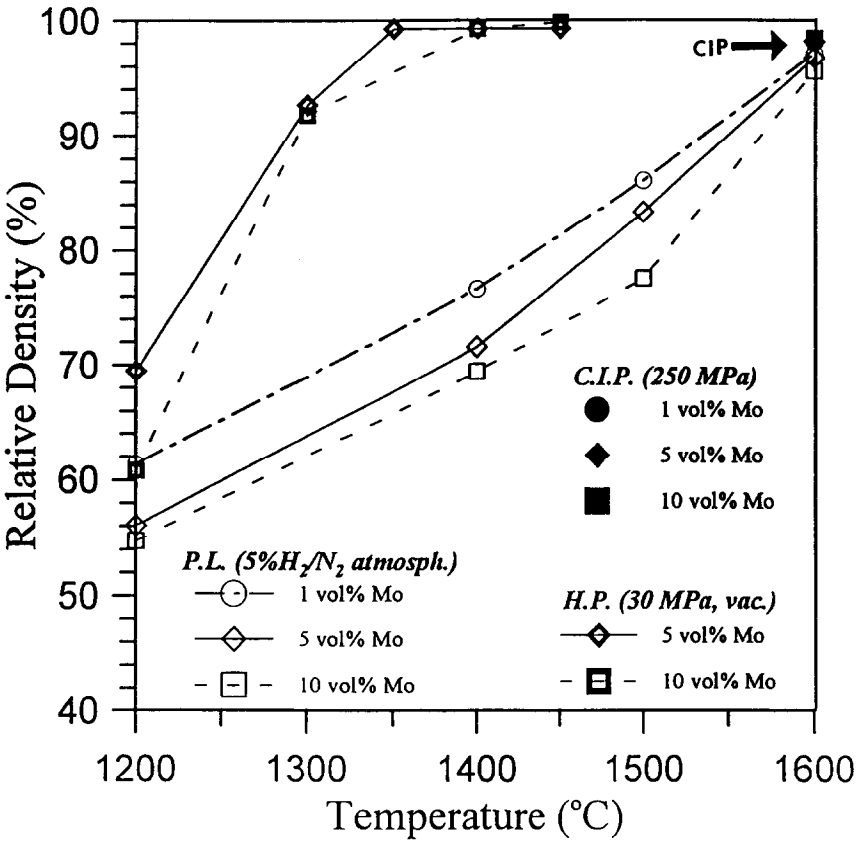

Figure 7. Relative density of sintered Mo/Al_2O_3 composites with various molybdenum contents. The composites were die-pressed or CIP, then sintered either by pressureless or hot pressed at 25 MPa for 1 hr.

The microstructure of three densified composites are shown in Figure 8. The Mo/Al_2O_3 composites were hot-pressed for 1 hr either at 1350°C (Figure 8(a)), 1450°C (Figure 8(b)); or sintered at 1600°C for 1 hr in a $5\%H_2/N_2$ atmosphere (Figure 8(c)). The Mo phase shows a darker contrast and uniform distribution in the alumina matrix.

The average grain sizes of Al_2O_3 and Mo are reported in Table 2. The sizes of alumina reduce with the increase of Mo content, basically follow the prediction of the Zener equation (16). The Mo grains are greater in size as the volume content of Mo increases. Large Mo grains are locate primarily at grain boundaries of Al_2O_3. Those Mo grains with sizes less than 0.2 μm are mostly enclosed in Al_2O_3 grains, as shown in Figure 8, and are spherical in shape. The discussion on various grain growth mechanisms in the Mo/Al_2O_3 composites will be presented in the other article (22).

Figure 9 shows two high resolution TEM micrographs illustrating the atomic structures near the interface between intragranular Mo/Al_2O_3 which are prepared from hot-pressed and fully densified composites. There are two types of interfacial structures resolved by HRTEM. One

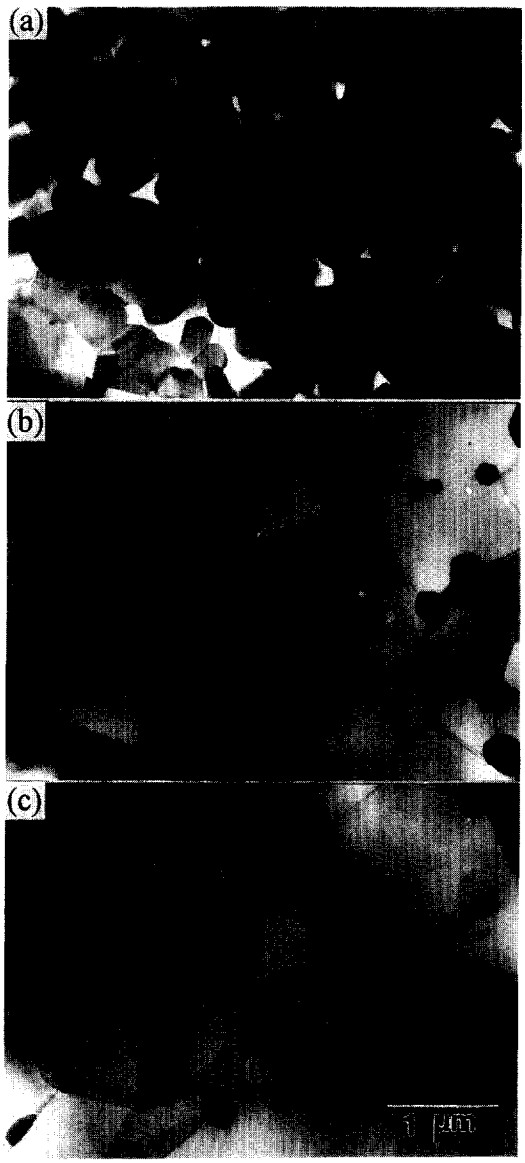

Figure 8. TEM micrographs of polished 10 vol% Mo/Al_2O_3 hot-pressed for 1 hr at (a) 1300° C, (b) 1450°C; or (c) die-pressed, then CIPed and pressurelessly sintered at 1600°C for 1 hr in $5\%H_2/N_2$ atmosphere.

(Figure 9(a)) appears a tilted interface of which only one or two layers of atoms are randomly arranged. The interface is as thin as 0.3 nm and depicts a non-coherent character. There is no glassy or intermediate phase at the interfaces of Mo/Al_2O_3. Most of the observed interfaces of the Mo/

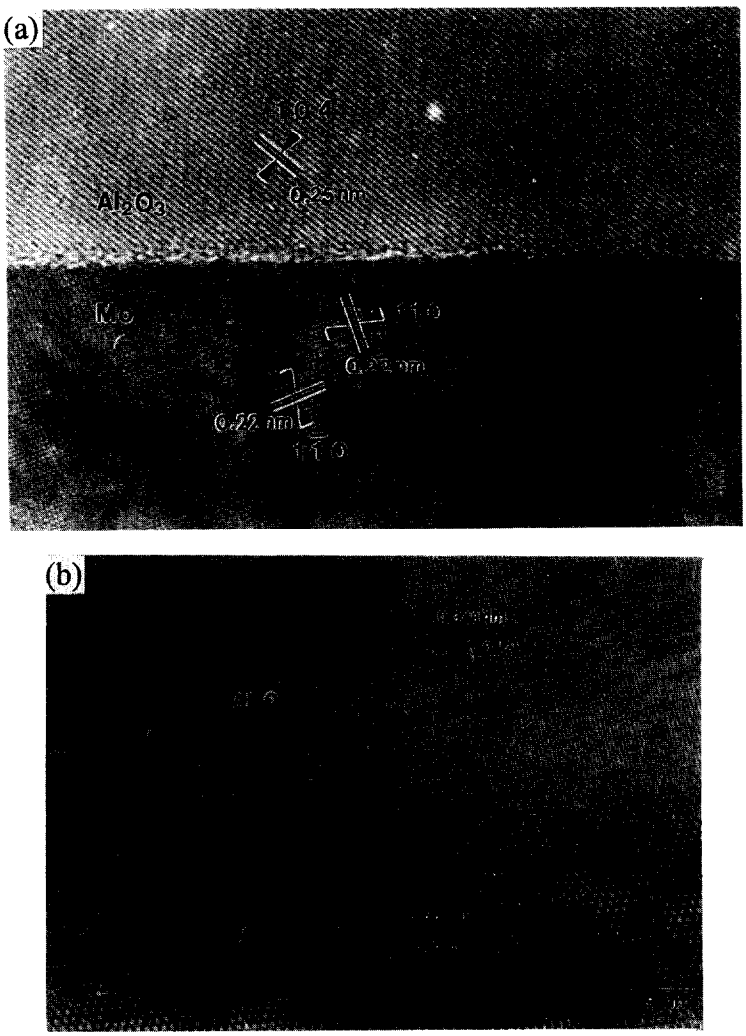

Figure 9. High resolution TEM micrograph of two atomic images near the interfaces of Mo (BCC) and Al_2O_3 (HCP) grains. (a) a non-coherent interface (b) a coherent interface.

Al_2O_3 belong to incoherent. However, there is one interface appearing as a fully coherent character, as shown in Figure 9(b). The coherency of the atomic images through the interface of Mo/Al_2O_3 is evident. The investigation of the lattice constant of the Al_2O_3 (012) plane and Mo (110), (112) planes reveals that the lattice spacing of $(012)_{Al203}$ is 0.348 nm, which is nearly equal to that of five layers of $(332)_{Mo}$. [Note: Only 3.4% difference to the lattice spacing of 0.336 nm which is five layers of $(332)_{Mo}$).] The vector of 332, as shown in the Mo atomic image (lower-right corner) of Figure 11(b), is a combination of 2x110 and 112 vectors. Therefore, the interface is coherent. In other words, $(332)_{Mo}//(012)_{Al2O3}$ can be existing at the interface of Mo/Al_2O_3.

4. CONCLUSION

A dissolution-precipitation method for the preparation of the mixtures of alumina ceramic slurry and ammonium molybdate solution, followed by a spray-drying process to obtain well-mixed Mo/Al_2O_3 precursory powders was demonstrated. The spray-dried powders were spherical in shape and had a wide size distribution with an average diameter ranging of about 4.8 μm. The spherical granules have ultrafine Mo grains in the sizes (30 nm to 0.4 μm) after a hydrogen reduction treatment from 600°C to 900°C. The Mo phase in the granules would grow in size during the heat treatment by a surface diffusion controlled mechanism, and would perform with a time dependent behavior. The time exponent (n) and activation energy of the grain growth process are 7 to 8 and 200 kJ/mol, respectively.

Spray-dried powder can be either hot-pressed to full density while hot-pressed at the temperatures higher than 1350°C (with ≤10 vol% Mo) or sintered at 1 atm and 1600°C for 1 h. The microstructure of densified composites shows a uniform distribution of the Mo-phase and having grain sizes of less than 0.5 μm. In addition, the matrix Al_2O_3 remains in submicrometric size. The interface between Mo and Al_2O_3 is clean and no glassy layer is found at the interfaces. Most of the interfaces are incoherent. Only one coherent interface, $(332)_{Mo}//(012)_{Al2O3}$, is identified between Mo/Al_2O_3.

ACKNOWLEDGMENT

The authors like to thank the funding from National Science Council in Taiwan contract number NSC87-22 1 6-E-002034.

REFERENCE

1. McHugh, C.O., Whalen, T.J. and Humenik, M., Jr., *Journal of the American Ceramic Society*, 1966, 49, 486.
2. Simpson, L.A. and Wasylyshyn, A., *Journal of the American Ceramic Society*, 1971, 54, 56.
3. Edelson, L.H. and Glaeser, A.M., *Communications of the American Ceramic Society*, 1988, 71, C-198.
4. Rankin, D.T., Stiglich, J.J., Petrak, D.R. and Ruh, R., *Journal of the American Ceramic Society*, 1971, 54, 277.
5. Nawa, M., Sekino, T. and Niihara, K., *Journal of Materials Science*, 1994, 29, 3185.
6. Waku, Y., Suzuki, M., Oda, Y. and Kohtoku, Y., *Journal of the Ceramic Society of Japan*, 1995, 103, 713.
7. Mayo, M.J., *Synthesis and Application of Nano-crystalline Ceramics*, Research Report, Center for Advanced Materials, Penn State Newsletter, 1993, Vol. 7, no. 1.
8. Stearns, L.C., Zhao, J. and Harmer, M.P., *Journal of the European Ceramic Society*, 1992, 10, 473.
9. Durrant, P.J. and Durrant, B., *Introduction to Advanced Inorganic Chemistry*, 1961, 2nd edition, p. 1030.
10. Funaki, K. and Segawa, T., *Journal of the Electro-Chemical Society of Japan*, 1950, 18, 152.
11. Lukasiewicz, S.J., *Journal of the American Ceramic Society*, 1989, 72, 617.
12. Wei, W.J., Lu, S.J. and Hsieh, C.L., *Journal of the Ceramic Society of Japan*, 1996, 104, 277.
13. Messing, G.L., Zhang, S.-Ch. and Jayanthi, G.V., *Journal of the American Ceramic Society*, 1993, 76, 2707.

14. Cheng, F.H., *Study on the Spray-Dried and Sintered Mo-Ceramic Composites*, Masters Thesis, National Taiwan University, 1996.
15. Wurst, J.C., Nelson, J.A., *Journal of the American Ceramic Society*, 1972, 55, 109.
16. Zener, C., as communicated by J.E. Burke, *Transactions of AIME*, 1949, 180, 73.
17. Luthra, N.P. and Cheng, W.-C., *Journal of Catalysis*, 1987, 107, 154.
18. Hunter, R.J., *Foundations of Colloidal Science*, Clarendon Press, Oxford, Vol. II, p. 756.
19. Chiang, Y.M., Birnie, D. III and Kingery, W.D., *Physical Ceramics*, John Wiley and Sons, Inc., 1997.
20. Coblenz, W.S., Dynys, J.M., Cannon, R.M. and Coble, R.L., *Proceedings of the 5th International Conference on Sintering and Related Phenomena*, ed. Kuczynski, Plenum Pres, NY, 1983.
21. Sloczynski, J. and Bobinski, W., *Journal of Solid State Chemistry*, 1991, 92, 436.
22. Wang, S.-C. and Wei, W.-C.J., *Characterization of Al_2O_3-Composites with Fine Mo Particulates, II. Densification and Mechanical Properties*, to be submitted to Nanostructured Materials.